Eur Biophys J (2011) 40:565–576
DOI 10.1007/s00249-011-0680-9

ORIGINAL PAPER

The presence of membranes or micelles induces structural changes of the myristoylated guanylate-cyclase activating protein-2

Stephan Theisgen · Lars Thomas · Thomas Schröder · Christian Lange · Michael Kovermann · Jochen Balbach · Daniel Huster

Received: 29 October 2010 / Revised: 20 January 2011 / Accepted: 25 January 2011 / Published online: 17 February 2011

Abstract Guanylate cyclase-activating proteins (GCAPs) are neuronal Ca^{2+} sensors that play a central role in shaping the photoreceptor light response and in light adaptation through the Ca^{2+}-dependent regulation of the transmembrane retinal guanylate cyclase. GCAPs are N-terminally myristoylated, and the role of the myristoyl moiety is not yet fully understood. While protein lipid chains typically represent membrane anchors, the crystal structure of GCAP-1 showed that the myristoyl chain of the protein is completely buried within a hydrophobic pocket of the protein, which stabilizes the protein structure. Therefore, we address the question of the localization of the myristoyl group of GCAP-2 in the absence and in the presence of lipid membranes as well as DPC detergents (as a membrane substitute amenable to solution state NMR). We investigate membrane binding of both myristoylated and nonmyristoylated GCAP-2 and study the structure and dynamics of the myristoyl moiety of GCAP-2 in the presence of POPC membranes. Further, we address structural alterations within the myristoylated N-terminus of GCAP-2 in the presence of membrane mimetics. Our results suggest that upon membrane binding the myristoyl group is released from the protein interior and inserts into the lipid bilayer.

Keywords Lipid modification · GCAP-2 · Membrane-protein interaction · Order parameter

Abbreviations

GC	Guanylate cyclase
GCAP-2	Guanylate cyclase-activating protein-2
NCS	Neuronal calcium sensor
HSQC	Heteronuclear single quantum coherence
POPC	1-Palmitoyl-2-oleoyl-*sn*-glycero-3-phosphocholine
DPC	Dodecylphosphocholine
IPTG	Isopropyl β-D-1-thiogalactopyranoside
OD	Optical density
GMP	Guanosine-5′-monophosphate
cGMP	Cyclic GMP
GTP	Guanosine-5′-triphosphate
EDTA	Ethylenediaminetetraacetic acid
HPLC	High performance liquid chromatography
FID	Free induction decay
TFA	Trifluoroacetic acid
INEPT	Insensitive nuclei enhanced by polarization transfer
DTT	Dithiothreitol
MOPS	3-(N-morpholino)propanesulfonic acid
MES	2-(N-morpholino)ethanesulfonic acid
Tris	Tris(hydroxymethyl)aminomethane
HEPES	4-(2-hydroxyethyl)-1-piperazineethanesulfonic acid

Membrane-active peptides: 455th WE-Heraeus-Seminar and AMP 2010 Workshop.

S. Theisgen · L. Thomas · D. Huster (✉)
Institute of Medical Physics and Biophysics,
University of Leipzig, Härtelstr. 16-18, 04107 Leipzig, Germany
e-mail: daniel.huster@medizin.uni-leipzig.de

T. Schröder · C. Lange
Institute of Biochemistry/Biotechnology,
Martin-Luther-University Halle-Wittenberg,
Kurt-Mothes-Str. 3, 06120 Halle (Saale), Germany

M. Kovermann · J. Balbach
Biophysics Research Group, Martin-Luther-University
Halle-Wittenberg, Betty-Heimann-Strasse 7,
06120 Halle (Saale), Germany

PDB	Protein databank
NMR	Nuclear magnetic resonance
MWCO	Molecular weight cut-off
TCEP	Tris(2-carboxyethyl)phosphine
WATERGATE	Water suppression by gradient-tailored excitation
GARP	Globally optimized alternating phase rectangular pulse
WALTZ	Wideband alternating-phase low-power technique for zero-residual-splitting
Cmc	Critical micelle concentration

Introduction

Guanylate cyclase-activating proteins (GCAP) are retinal Ca^{2+} sensors. So far, three members of the family have been found in vertebrates (GCAP-1 through GCAP-3) (Dizhoor et al. 1995; Frins et al. 1996; Gorczyca et al. 1994) and five additional genes (GCAP-4 through GCAP-8) were identified or predicted in zebrafish and pufferfish (Imanishi et al. 2004). GCAPs play a central role in shaping the photoreceptor light response and in light adaptation through the Ca^{2+}-dependent regulation of the retinal transmembrane guanylate cyclase (GC) (Dizhoor et al. 1995). They belong to the family of neuronal calcium sensor (NCS) proteins and therefore to the superfamily of EF-hand Ca^{2+}-binding proteins (Burgoyne and Weiss 2001). Like most other NCS proteins, GCAPs are N-terminally myristoylated (Demar et al. 1999). Lipid modifications often serve as membrane anchors (Brunsveld et al. 2009; Casey 1995). Although a single lipid modification does not seem to be sufficient for stable membrane binding of a protein (Peitzsch and McLaughlin 1993), it has been shown for some NCS that they bind to the membrane via their myristoyl moiety, typically assisted by additional electrostatic interactions or the insertion of hydrophobic residues into the bilayer.

The interaction between NCS proteins and the membrane is often tightly regulated. For the NCS prototype protein recoverin, this regulation mechanism is called the Ca^{2+}-myristoyl switch (Zozulya and Stryer 1992). It was shown that in the Ca^{2+}-free state, the myristoyl moiety is buried inside the hydrophobic core, which renders the molecule soluble. Upon Ca^{2+} binding, the myristoyl chain is released from the protein and exposed to the medium, which directs the molecule to the membrane. Such a mechanism was also observed for neurocalcin δ and hippocalcin (Kobayashi et al. 1993; Ladant 1995), but not for NSC-1, which shows a Ca^{2+}-indepedent membrane binding (McFerran et al. 1999).

For the GCAPs, the role of the myristoyl moiety is not fully understood. So far, most reports conclude that no Ca^{2+}-myristoyl switch exists for the GCAPs (Hughes et al. 1998; Hwang and Koch 2002b; O'Callaghan and Burgoyne 2004; Olshevskaya et al. 1997). In addition to the putative function as membrane anchor, some studies tested the structural and mechanistic influence of the myristoylation on GC activation. Comparative studies between myristoylated and nonmyristoylated GCAPs revealed that for GCAP-2 myristoylation has no influence on the affinity for the GC-1, but myristoylated GCAP-1 shows a sevenfold higher affinity for the GC-1 (Hwang and Koch 2002b). The myristoylated form of GCAP-2 is a more effective activator of the GC, although myristoylation is not required for GC activation (Hwang and Koch 2002b; Olshevskaya et al. 1997).

On the structural side, our own work has shown that the myristoyl moiety of GCAP-2 (Vogel et al. 2007a) and that of an N-terminal myristoylated peptide comprising the first 19 amino acids of GCAP-2 (Theisgen et al. 2010) are membrane inserted in disaturated DMPC host membranes as well as in more physiological monounsaturated quaternary lipid mixtures. In fact, the myristoyl moiety also showed structure and dynamics very similar to the lipid chains of the host membrane. This is in very good agreement with many lipid-modified proteins that have been investigated by ^2H solid-state NMR such as Ras (Reuther et al. 2006; Vogel et al. 2007b; Vogel et al. 2009), Src (Scheidt and Huster 2009), or SP-C (Gonzales-Horta et al. 2008). Therefore, all previous work would strongly suggest that the lipid chain of GCAP-2 is inserted into the membrane. As there is apparently no Ca^{2+}-myristoyl switch mechanism for either GCAP-1 or GCAP-2 (Hwang and Koch 2002a; Olshevskaya et al. 1997), one would consequently have to assume that the myristoyl chain is exposed to the surface of the protein, perhaps facing a somewhat hydrophobic cluster of amino acids (Hughes et al. 1998).

However, the crystal structure of Ca^{2+}-bound GCAP-1 showed that the myristoyl chain of the protein is completely buried within a hydrophobic pocket of the protein created at the interface between the N- and C-termini (Stephen et al. 2007). This structural arrangement was found to provide hydrophobic interactions to further stabilize the structure of GCAP-1, as was hypothesized earlier (Olshevskaya et al. 1997). All other structural data on GCAP homologs have been obtained in the absence of the myristoyl chain (Ames et al. 1999; Stephen et al. 2006).

This quite surprising result may bring a myristoyl chain switch mechanism—perhaps not necessarily Ca^{2+} regulated—back into the picture because one should not forget that in vivo GCAPs are typically membrane-associated. The proximity of the membrane could possibly induce an extrusion of the myristoyl moiety from the hydrophobic

core into the hydrophobic membrane interior. Nevertheless, Ca^{2+}-dependent conformational changes of GCAP-2 have also been discussed in literature (Hughes et al. 1998).

A further increase in complexity comes from the fact that GCAP-2 binds to the membrane both in the presence and in the absence of the myristoyl moiety (Olshevskaya et al. 1997). The difference in binding energy is only on the order of k_BT (Vogel et al. 2007a), and the GCAPs are membrane-associated both in the Ca^{2+}-free and in the Ca^{2+}-bound states (Olshevskaya et al. 1997).

In this study, we address the question of the localization of the myristoyl group of GCAP-2 in the absence and in the presence of lipid membranes as well as DPC detergents (as a membrane substitute amenable to solution state NMR). We investigate membrane binding of both myristoylated and nonmyristoylated GCAP-2 and study the structure and dynamics of the myristoyl moiety of GCAP-2 in the presence of POPC membranes. Furthermore, we study structural changes within the myristoylated N-terminus of GCAP-2 in the presence of membrane mimetics. Based on these data and the findings from literature, we finally suggest a model for membrane binding of GCAP-2.

Materials and methods

Materials

1-Palmitoyl-2-oleoyl-*sn*-glycero-3-phosphocholine (POPC) and 1-palmitoyl-d_{31}-2-oleoyl-*sn*-glycero-3-phosphocholine (POPC-d_{31}) were purchased from Avanti Polar Lipids (Alabaster, AL, USA), and dodecylphosphocholine-d_{38} was purchased from Cambridge Isotope Laboratories (Andover, MA, USA).

Protein synthesis

GCAP-2 was expressed in *Escherichia coli* BL21(DE3) using a pET-11a expression vector coding for bovine GCAP-2 (Hwang and Koch 2002a). Myristoylation was achieved by coexpressing the yeast N-myristoyl transferase I encoded by the plasmid pBB131 and adding myristic acid to the growth medium (Duronio et al. 1990; Hwang and Koch 2002b). Isotopically labeled GCAP-2 was produced in a fed-batch process on a slightly modified version of the defined salt medium described by Korz et al. (1995). The final composition was 13.3 g/l KH_2PO_4, 4.3 g/l Na_2HPO_4, 1.2 g/l $MgSO_4{\cdot}7H_2O$, 1.7 g/l citrate·H_2O, 8.4 mg/l EDTA, 2.5 mg/l $CoCl_2{\cdot}6H_2O$, 1.5 mg/l $CuCl_2{\cdot}2H_2O$, 3.0 mg/l H_3BO_3, 2.5 mg/l $Na_2MoO_4{\cdot}2H_2O$, 13.0 mg/l $Zn(CH_3COO)_2{\cdot}2H_2O$, 100.0 mg/l Fe(III)citrate·H_2O with a pH of 6.7. The medium contained $^{15}NH_4Cl$ (3.24 g/l) as nitrogen source. The same amount was added to the culture at an OD_{600} of about 12 and again directly after induction. As the carbon source, 20 g/l glucose was present in the initial medium and supplemented as needed after the initial amount was exhausted. For ^{13}C labeling, uniformly ^{13}C-labeled glucose was added after the initial glucose was metabolized. During the whole fermentation, the temperature (37°C) and the pH (6.7) were kept constant. Myristic acid (either protonated or deuterated) dissolved in ethanol was fed continuously for 2 h (start 30 min before induction) or added manually 30 min before induction and again 1 h after induction. For ^2H labeling, 50% of the H_2O in the fermentation medium was replaced by D_2O. Expression of GCAP-2 was induced by adding 1 mM IPTG. The cells were harvested 4 h after induction.

The inclusion bodies were isolated following standard procedures (Rudolph et al. 1997). The solubilized inclusion bodies (10–20 mg/ml protein in solubilization buffer: 6 M guanidinium chloride, 100 mM Tris-HCl pH 8.0, 1 mM EDTA, 100 mM DTT) were rapidly diluted (about 100-fold) by dropwise addition to stirred ion exchange chromatography buffer A (20 mM HEPES pH 8.0, 20 mM NaCl, 1 mM $CaCl_2$). Protein concentration during refolding was between 100 and 150 µg/l. After at least 4 h the suspension was cleared by centrifugation and filtration, and subsequently loaded onto a HiTrap Q Sepharose HP anion exchange column (Amersham Biotech, Little Chalfont, UK) at a flow of 5 ml/min. The elution was performed by a linear gradient from buffer A to buffer B (20 mM HEPES pH 8.0, 1 M NaCl, 1 mM $CaCl_2$) or by step elution with 29% of buffer B. The fractions containing GCAP-2 were pooled and further purified by C18 reversed-phase HPLC (Column: VP250/10 NUCLEOSIL 300-5 C18 from Macherey-Nagel, Düren, Germany) with a linear gradient of water to acetonitrile, both containing 0.1% TFA. During this step, myristoylated GCAP-2 (~80%) was separated from the nonmyristoylated form (~20%). The eluent was removed by evaporating it in a Jouan RC 10.22 vacuum concentrator (Jouan, Saint Mazaire, France). The remaining pellet was then dissolved in solubilization buffer, and the protein was refolded by dropwise rapid dilution (more than 100-fold) into the refolding buffer (100 mM Tris pH 8.0–8.5, 500 mM Na_2SO_4, 1 mM $CaCl_2$, 1–2 mM DTT); no precipitation was observed. The solution was then concentrated by cross flow filtration (using a Vivaflow 200 from Sartorius, Göttingen, Germany) or by ultrafiltration (with regenerated cellulose membranes, MWCO 10 kDa, from Millipore, Billerica, MA, USA) to 30–50 ml, afterwards dialyzed against the final measurement buffer and then concentrated further by centrifugal ultrafiltration (using Amicon Ultracel-3 K from Millipore) to the required final concentration.

Binding measurements

POPC was suspended in measurement buffer (20 mM MES pH 6.0, 50 mM Na_2SO_4, 1 mM $CaCl_2$, 1 mM TCEP) to a concentration of 10 mM. After 10 freeze-thaw cycles, the solution was extruded at least 10 times through two polycarbonate filters of 100 nm pore size (Millipore) at 37°C using a LIPEX thermo stated extruder (Biomembranes, Vancouver, BC, Canada) (Hope et al. 1985), obtaining 100 nm unilamellar vesicles (LUVs). A phosphate assay (Chen et al. 1956) was performed to determine the final concentration of POPC (7.4 ± 0.4 mM). The protein sample was prepared as described above; the final assay protein concentration was 0.65 μM for myristoylated GCAP-2 and 0.57 μM for nonmyristoylated GCAP-2.

Tryptophan fluorescence spectra were acquired on a Fluoromax 2 spectrometer (Jobin-Yvon, Edison, NJ, USA), using 290 nm as excitation wavelength, and emission was observed between 300 and 470 nm. Aliquots of the liposome dispersion were titrated to the protein solution. Fluorescence intensities at 348 nm were used for the calculation of membrane-bound fraction of the protein, according to Ladokhin et al. (2000):

$$f_b = \frac{I - I_0}{I_\infty - I_0}, \tag{1}$$

where f_b denotes the membrane-bound fraction, I is the fluorescence intensity, I_0 is the fluorescence intensity in the absence of lipid, and I_∞ is the fluorescence intensity that corresponds to complete binding. This value (I_∞) is unknown and has to be determined from the fit to the recorded data.

From the binding curve, the Gibbs free energy of the transfer from the aqueous solution to the membrane can be determined directly (Ladokhin et al. 2000):

$$I([L]) = I_0 + (I_\infty - I_0)\frac{k[L]}{[W] + k[L]}, \tag{2}$$

where [L] is the lipid concentration, k the mole-fraction (X) partition coefficient ($k = X_{bilayer}/X_{water}$), and [$W$] the concentration of water (55.5 M). The respective K_D value can be determined from the mole-fraction partition coefficient ($K_D = [W]/k$) (White and Wimley 1999). Then, the standard Gibbs free energy (ΔG^0) of membrane binding can be calculated according to White and Wimley (1999):

$$\Delta G^0 = -RT \ln k. \tag{3}$$

Sample preparation for ^{2}H solid-state NMR

POPC was suspended in buffer (20 mM MES pH 6.0, 50 mM Na_2SO_4, 0.5 mM TCEP). After freeze-thawing and extrusion, large unilamellar vesicles (LUVs) with a diameter of 100 nm were obtained. The protein solution was dialyzed against the same buffer (for the sample containing Ca^{2+}, 5 mM $CaCl_2$ was added, and for the sample containing no Ca^{2+} but Mg^{2+}, the buffer was supplemented with 10 mM $MgCl_2$ and 2 mM EGTA), added to the liposome suspension, and incubated overnight at 37°C. The molar ratio of protein to lipid was 1:150. The samples were lyophilized and hydrated with 50 wt% H_2O. For equilibration, the sample was frozen, thawed, stirred, and gently centrifuged several times.

^{2}H solid-state NMR spectroscopy

All ^{2}H experiments were carried out on a Bruker Avance 750 NMR spectrometer (Bruker, Rheinstetten, Germany) operating at a resonance frequency of 115.1 MHz for ^{2}H. The ^{2}H NMR spectra were acquired at 30°C using a phase-cycled quadrupolar echo pulse sequence (^{2}H 90° pulse length: 2.1–2.3 μs, inter-pulse delay: 60 μs, relaxation delay: 0.7–0.8 s) (Davis et al. 1976). ^{2}H NMR spectra were dePaked, and smoothed chain order parameters were calculated (Lafleur et al. 1989). The Pake doublets were assigned to the carbons consecutively according to their increasing quadrupolar splitting. A more detailed description of the procedure can be found in the literature (Huster et al. 1998; Vogel et al. 2007a).

Solution NMR spectroscopy

All ^{1}H NMR spectra were recorded on a Bruker DRX600 MHz spectrometer using a 5-mm triple-inverse broadband probehead with z-gradients. A standard single pulse excitation pulse sequence using a WATERGATE W5 sequence with gradient support for water suppression (Liu et al. 1998) was used, applying a GARP decoupling scheme for ^{15}N decoupling during acquisition.

All ^{1}H-^{15}N HSQC spectra were recorded at 40°C using the standard pulse program consisting of a double INEPT transfer, with sensitivity improvement, decoupling during acquisition and trim pulses (Kay et al. 1992; Palmer et al. 1991; Schleucher et al. 1994). In the titration experiments, 80 transients with 176 data points in the indirect dimension (acquisition time of 32 ms) with a relaxation delay of 1 s were recorded. Several DPC stock solutions were prepared in the same buffer the protein was dissolved in (20 mM MES, 50 mM Na_2SO_4, 5 mM $CaCl_2$, 10 mM DTT, pH 6.0 with 10% D_2O), and titration was carried out by successively adding aliquots of the appropriate stock solution and subsequent mixing. Thirteen titration points with a final DPC concentration of 69.6 mM were measured.

The ^{1}H-^{15}N HSQC spectra measured for comparison of the myristoylated and nonmyristoylated form in the presence and absence of 20 mM DPC were recorded with

slightly better resolution and signal to noise (152 scans and 256 data points in the indirect dimension, yielding an acquisition time of 47 ms). The buffer conditions were the same as in the titration experiments, except that only 2 mM $CaCl_2$ and 2 mM DTT were used.

Triple resonance spectra and partial assignment

All NMR spectra were recorded at 35°C, with a final protein concentration of ~430 μM in measurement buffer (20 mM MES pH 6.0, 50 mM Na_2SO_4, 20 mM DPC, 5 mM $CaCl_2$, 10 mM DTT) containing 5% D_2O. Spectra were processed using NMRpipe (Delaglio et al. 1995). For the backbone resonance assignments, trHNCA, trHNCACB, and trHN(CO)CACB spectra of a $^{15}N/^{13}C/^{2}H$-labeled sample were acquired with a Bruker Avance III 800 spectrometer equipped with a cryoprobe. Deuterium decoupling during ^{13}C chemical shift evolution was achieved by WALTZ-16.

Results

Liposome binding data

Although the crystal structure of GCAP-1 (Stephen et al. 2007) showed the myristoyl group buried inside the protein, it is reported that the molecule is membrane-associated, and previous data on GCAP-2 have shown that the lipid chain is inserted into DMPC bilayers (Vogel et al. 2007a). In order to gain more insight about a possible membrane insertion of the myristoyl chain of GCAP-2, we carried out binding measurements of myristoylated and nonmyristoylated GCAP-2 to POPC membranes, monitored by Trp fluorescence intensity alterations shown in Fig. 1.

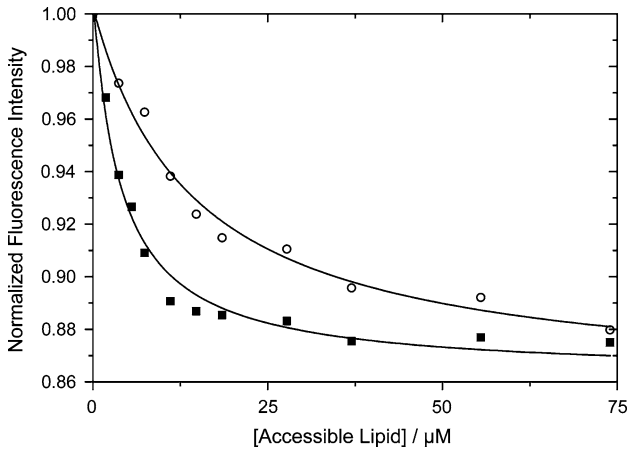

Fig. 1 Fluorescence intensity changes for myristoylated (*filled square*) and nonmyristoylated GCAP-2 (*open circle*) induced by titration of 100 nm POPC liposomes. The *solid lines* represent the prediction of the binding model according to Eqs. 1–3

Indeed, quite different binding data were measured. The K_D for the myristoylated GCAP-2 was 4.1 ± 0.6 μM, while nonmyristoylated GCAP-2 showed much weaker binding (K_D = 14.5 ± 2.5 μM). However, this difference only resulted in a $\Delta\Delta G^0$ of −3.2 kJ/mol (ΔG^0 = −40.2 kJ/mol for the myristoylated GCAP-2 and ΔG^0 = −37.0 kJ/mol for the nonmyristoylated protein, respectively), while a difference on the order of −25 to −30 kJ/mol was expected (see "Discussion").

^{2}H solid-state NMR spectroscopy of myristoylated GCAP-2

In order to measure whether or not the myristoyl chain of GCAP-2 was inserted into the bilayer when the molecule was bound to the membrane, we carried out ^{2}H solid-state NMR experiments on the deuterated myristoyl chain of GCAP-2 and compared them with the ^{2}H NMR spectra for the host membrane. Typical NMR spectra are shown in Fig. 2.

As a reference, we measured the ^{2}H NMR spectrum of pure POPC-d_{31} membranes (Fig. 2a), which showed the characteristic superposition of Pake doublets measured for deuterated lipid or protein chains (Seelig and Seelig 1980). The maximum quadrupolar splitting was on the order of ~30 kHz and thus typical for lipid chains forming a liquid crystalline membrane. When GCAP-2 was bound to the POPC membrane, only marginal changes in the quadrupolar splittings were observed (Fig. 2b). However, the line width of the ^{2}H NMR spectrum of POPC in the presence of GCAP-2 was somewhat broader indicating the influence of protein binding causing slightly slower lipid motions. Even broader NMR signals were measured for the deuterated myristoyl moiety of GCAP-2-d_{27} both in the absence (Fig. 2c) and in the presence of 5 mM Ca^{2+} (Fig. 2d), which suggests slower motions of this protein-associated lipid chain compared to the phospholipids. This would agree with literature data on the Ras protein (Huster et al. 2003; Reuther et al. 2006; Vogel et al. 2005). For comparison, we also measured the NMR spectrum of GCAP-2-d_{27} in the absence of any membranes and hydrated to 50 wt% buffer as the other samples (Fig. 2e). This spectrum features an isotropic line with perhaps some broader background signals suggesting high mobility of the majority of the myristoyl protein chain.

As the spectrum of deuterated GCAP-2 in the absence of membrane deviated so significantly from that measured in the presence of membranes, the results already indicate that the myristoyl moiety of membrane-associated GCAP-2 was truly inserted into the bilayer. The ^{2}H NMR spectrum of deuterated GCAP-2 in the absence of Ca^{2+} (Fig. 2c) also showed a small isotropic peak indicating that a small fraction of the chain is in fast exchange between a free or protein-bound and a membrane-embedded state.

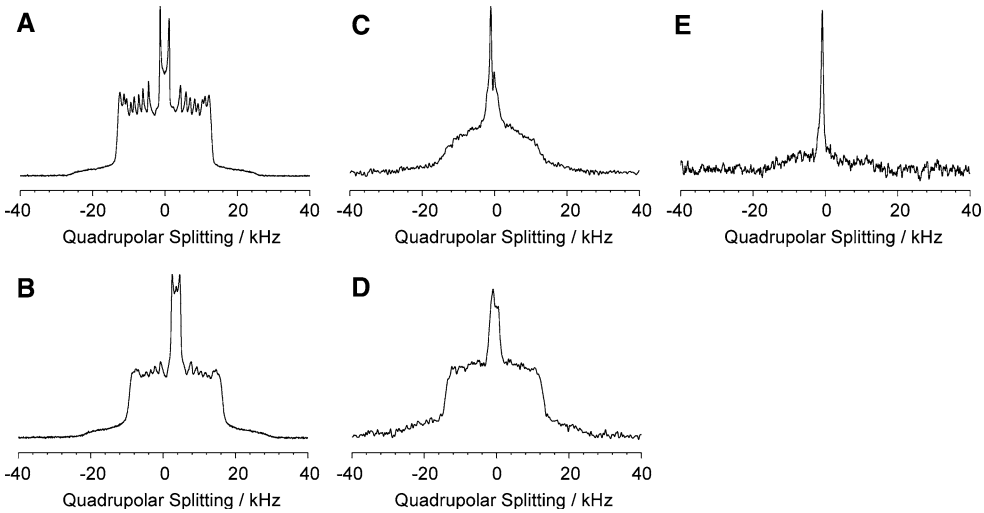

Fig. 2 The 115.1 MHz ^{2}H NMR powder spectra of POPC-d_{31} (**a**) and POPC-d_{31} in the presence of GCAP-2 (**b**). Further, the ^{2}H NMR spectra of myristoyl-deuterated GCAP-2 bound to POPC liposomes in the absence (**c**) and in the presence of 5 mM Ca^{2+} (**d**) are shown. The protein to lipid molar ratio was 1:150. **e** ^{2}H NMR spectrum of myristoyl-deuterated GCAP-2 in the absence of membranes. All spectra were recorded at a temperature of 30°C and a buffer content of 50 wt%

Next, for a more quantitative analysis, we converted the ^{2}H NMR spectra into smoothed chain order parameter plots (Lafleur et al. 1989) shown in Fig. 3. The presence of GCAP-2 in the membrane did not lead to any significant alterations of the lipid packing in the host membrane. Also, the order parameters of GCAP-2 in the presence and in the absence of Ca^{2+} were quite similar. Comparing the order parameter plots of the protein lipid chains with those of the host membrane, one finds that the protein chain order parameters at the beginning of the chains were slightly increased. Towards the end of the chain the order parameters of the POPC-d_{31} membrane decreased more slowly than the order parameters of the myristoyl moiety.

We further analyzed the ^{2}H NMR data using the mean-torque model for the acyl chain segment distributions

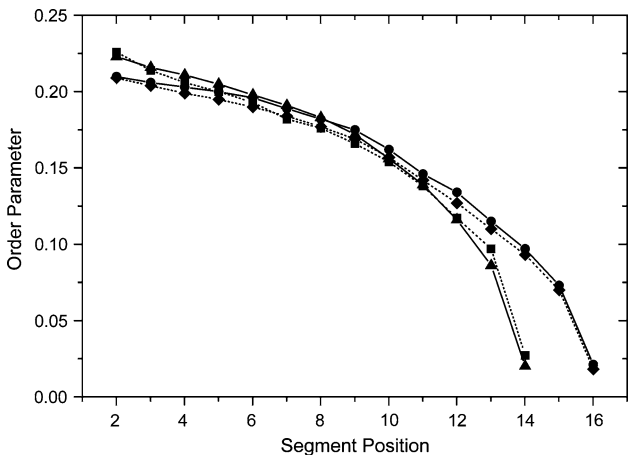

Fig. 3 Smoothed chain order parameters calculated from the ^{2}H NMR spectra shown in Fig. 2. Data refer to pure POPC-d_{31} membranes (*filled circle*), POPC-d_{31} membranes in the presence of GCAP-2 (*filled diamond*), and of myristoyl chain deuterated GCAP-2 in POPC liposomes in the absence (*filled square*) and in the presence of 5 mM Ca^{2+} (*filled triangle*). All data were recorded at a temperature of 30°C; the protein to lipid molar ratio was 1:150

(Petrache et al. 2000; Vogel et al. 2005). This allowed us to compare the chain extent of the membrane-inserted myristoyl moiety of GCAP-2 ($L_C^* = 10.2$ Å, both in the absence and in the presence of Ca^{2+}) with the length of the POPC-d_{31} host membrane ($L_C^* = 11.4$ Å). Apparently, there is a small chain length mismatch of 1.2 Å, which is strikingly similar to what has been found in literature for membrane-inserted Ras in POPC membranes (Vogel et al. 2009). This chain length difference contrasts the previously observed perfect length match seen for GCAP-2 in DMPC (Vogel et al. 2007a), which is, for the current example, most likely just a consequence of the difference between myristoyl and palmitoyl chains. Usually, the lipid chains tend to match the z-coordinate of the terminal methyl group in the middle of the bilayer in order to avoid chain interdigitation (Venable et al. 1993). This would mean that Gly 2, to which the myristoyl chain is attached, is slightly inserted into the membrane interface.

Structural differences between myristoylated and nonmyristoylated GCAP-2

As discussed above, the classical example for a Ca^{2+}-regulated switch mechanism is the NCS recoverin (Ames et al. 1997), which features the myristoyl chain inserted into the protein in the Ca^{2+}-free state but exposed to the aqueous environment in the Ca^{2+}-bound state. So far, no such mechanism has been reported for any member of the GCAP family (Hughes et al. 1998; Hwang and Koch 2002b; Olshevskaya et al. 1997).

The data available for recoverin suggest that significant structural alterations occur when the myristoyl moiety switches from the inside to the outside of the protein. Such structural changes can be very well observed in solution NMR spectra; in particular the amide proton region provides a characteristic fingerprint of the protein structure.

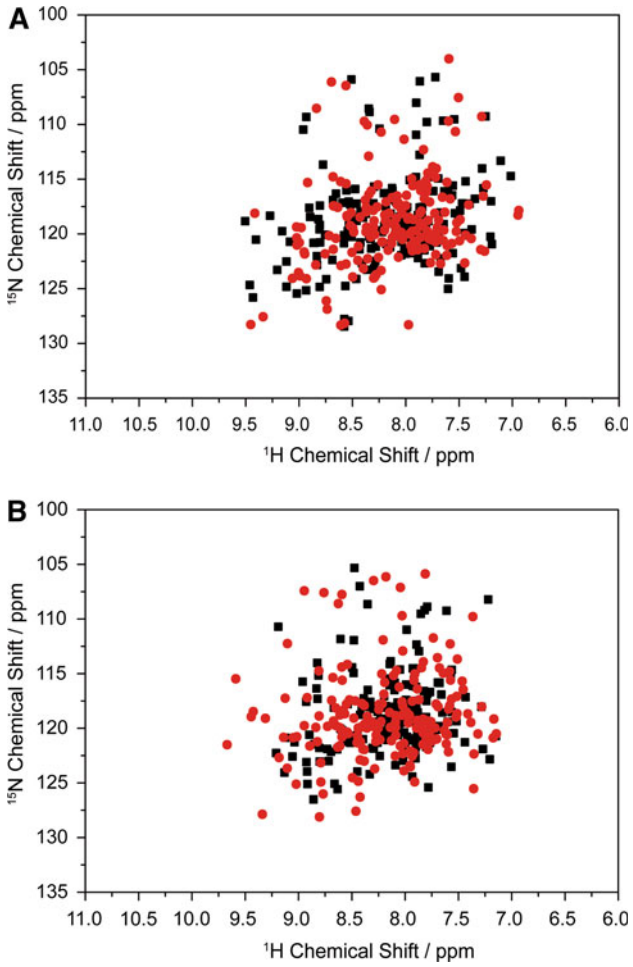

Fig. 4 Simulated ^{1}H-^{15}N HSQC spectra for **a** myristoylated recoverin in the presence (*black*; Ames et al. 1997) and in the absence of Ca^{2+} (*red*; Tanaka et al. 1995). **b** The points in the plot correspond to the chemical shifts of nonmyristoylated (*black*; Weiergraber et al. 2003) and myristoylated recoverin (*red*; Ames et al. 2002) both in the presence of Ca^{2+}. The chemical shifts were calculated from the protein structures using Sparta (Shen and Bax 2007)

To illustrate this, we have simulated the ^{1}H-^{15}N HSQC spectra for recoverin from the PDB entries using Sparta (Shen and Bax 2007). This simulation was necessary as NMR data are not available for all relevant proteins. However, using Sparta, NMR spectra could be predicted from the crystal structure.

The resulting theoretical NMR spectra are shown in Fig. 4. Figure 4a shows the calculated spectra for myristoylated recoverin in the absence (i.e., the chain buried state) and in the presence of Ca^{2+} (i.e., the chain exposed state), where significant chemical shift changes reflect the structural alterations associated with the myristoyl switch. In Fig. 4b, we compare the NMR spectra of both myristoylated and nonmyristoylated recoverin in the presence of Ca^{2+}, where the myristoyl moiety of recoverin is located inside the protein. Again, rather drastic chemical shift alterations are expected that reflect the structural differences between the two proteins. It should be noted that this comparison does not reflect all chemical shift changes observed in the experiment. In particular, the Ca^{2+}-bound EF-hands are not well predicted by Sparta. Nevertheless, as not all experimental NMR spectra are available from the literature, we think that this comparison may be instructive.

Although recoverin and GCAP-2 are rather different proteins, we applied a sequence homology analysis. This analysis showed 29.2% identity and 47.3% similarity. In order to test if chemical shift differences of a similar magnitude could be observed between the spectra of myristoylated and nonmyristoylated GCAP-2, we acquired ^{1}H-^{15}N HSQC spectra of myristoylated and nonmyristoylated GCAP-2, which are shown in Fig. 5. The signals are well dispersed as is typical for largely α-helical proteins. The NMR spectrum of the nonmyristoylated form is comparable, but not fully identical (we used slightly different buffer conditions), to the data published before (Ames et al. 1999).

Overall, the NMR spectra look fairly similar for myristoylated and nonmyristoylated GCAP-2, respectively. So far, we have not been able to obtain a complete assignment, but most amino acids of the N-terminus can be assigned. There are only moderate chemical shift differences in the N-terminus suggesting only small structural alterations induced by the presence of the myristoyl moiety. The signal of Gly 2 can only be detected in the myristoylated form of GCAP-2 since fast exchange prevents the detection of this signal in the nonmyristoylated protein.

Structural influence of DPC on myristoylated and nonmyristoylated GCAP-2

Next, we asked the question if more structural changes would be visible in the presence of lipid membranes. However, when liposomes are present, the solution NMR spectra of membrane-associated proteins usually deteriorate, caused by increased line widths up to a complete loss of resonances (Barre and Eliezer 2006). Therefore, we used the membrane-mimicking detergent DPC in order to investigate structural changes associated with a putative switch mechanism for the myristic acid moiety of GCAP-2. The ^{1}H-^{15}N HSQC spectra of myristoylated and nonmyristoylated GCAP-2 in the presence of 20 mM DPC are shown in Fig. 6.

Compared to the NMR spectra in the absence of DPC, the signal dispersion was somewhat lower. In the presence of DPC, the spectra of the myristoylated and the nonmyristoylated GCAP-2 were again very similar. Only a few differences could be seen, mostly for peaks that belonged to N-terminal amino acids. Pronounced chemical shift changes can be observed for Gln 4, Phe 5, Ser 6, Gly 14, Ala 15, Gly 17, and Ala 18.

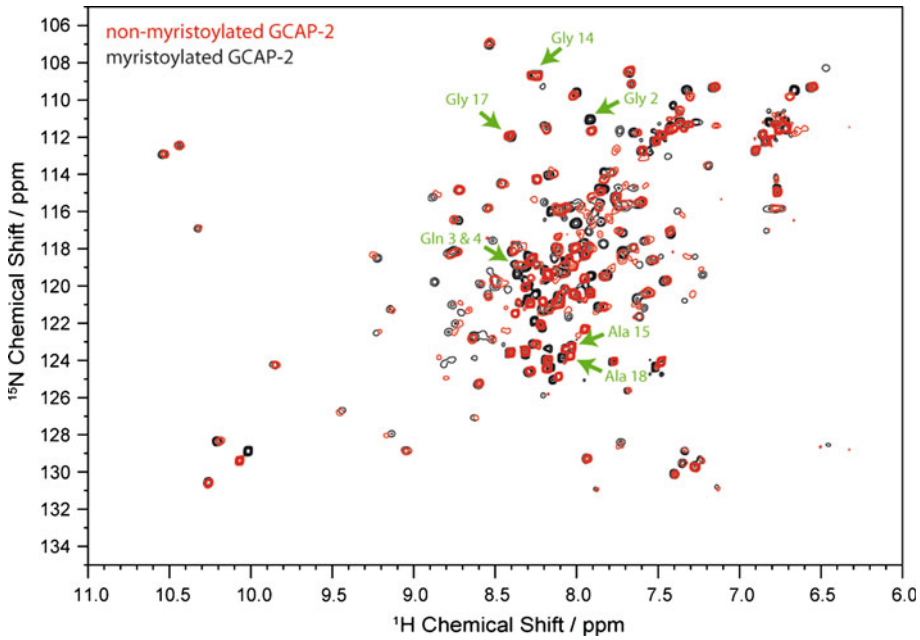

Fig. 5 ^{1}H-^{15}N HSQC spectra of myristoylated (*black*) and nonmyristoylated (*red*) GCAP-2, recorded at a temperature of 40°C. Assigned amino acids from the N-terminus are labeled and marked with *arrows*

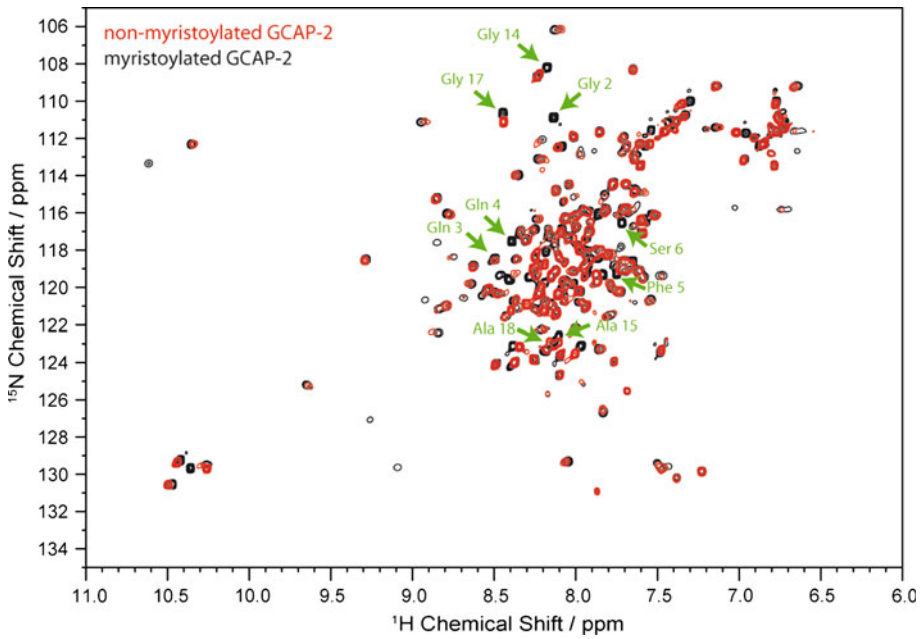

Fig. 6 ^{1}H-^{15}N HSQC spectra of myristoylated (*black*) and nonmyristoylated (*red*) GCAP-2 in the presence of 20 mM DPC, recorded at a temperature of 40°C. Assigned N-terminal amino acids are labeled and marked with *arrows*

To quantify the influence of DPC on the GCAP-2 structure, we performed titration experiments. In these experiments, the DPC concentration was increased stepwise from 0 to ~70 mM in 13 titration steps. For each titration point, a ^{1}H-^{15}N HSQC spectrum was recorded, and the weighted chemical shift difference $\Delta\delta$ was calculated according to Seo et al. (2010):

$$\Delta\delta = \sqrt{\left(\Delta\delta(^{1}H)\right)^{2} + \left(\Delta\delta(^{15}N)/5\right)^{2}}. \quad (4)$$

As seen from Fig. 6, the presence of DPC causes several peaks to shift. For the N-terminal amino acids we were able to assign, the peaks and the corresponding weighted chemical shift differences are shown in Fig. 7. The data points show a rather steep increase and a quick flattening out to reach the plateau value. Such titration results are typically in agreement with a K_D value far below 1 mM, which would also be the order of magnitude obtained in the fluorescence experiments for POPC. Such a K_D value would be below the critical micelle concentration (CMC) of DPC in water (1.5 mM), however, the CMC of DPC in the presence of GCAP-2 has not been determined.

We also compared the chemical shift difference between nonmyristoylated and myristoylated GCAP-2 in the

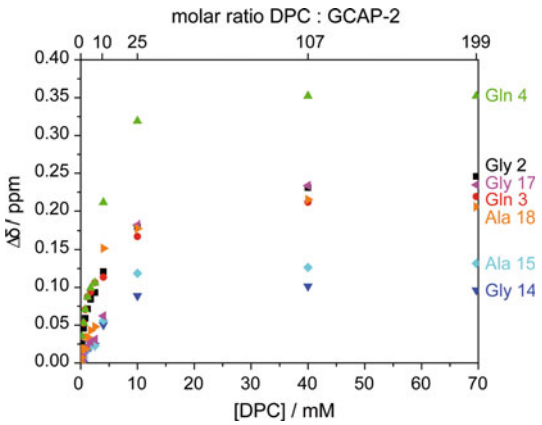

Fig. 7 Weighted chemical shift differences, $\Delta\delta$, for selected N-terminal amino acids, based on successively recorded ^{1}H-^{15}N HSQC spectra for the DPC titration to the myristoylated GCAP-2

absence and presence of DPC. This comparison shows that DPC has a more pronounced influence on the myristoylated form of GCAP-2, suggesting that more pronounced conformational changes occur for this form of the protein.

Discussion

In the present study, we address the apparent discrepancy between two previous experimental findings. First, using solid-state NMR spectroscopy, the lipid modification of GCAP-2 was found to be membrane inserted both for an N-terminal GCAP-2 peptide (Theisgen et al. 2010) and the full length GCAP-2 protein (Vogel et al. 2007a). Second, in contrast, the crystal structure of GCAP-1 showed this lipid chain to be completely buried in a hydrophobic pocket of the protein interior (Stephen et al. 2007), which was proposed to provide a "structure-stabilizing function" (Haynes and Burgoyne 2008).

A first approach to understanding these controversial results is to compare the binding energies of myristoylated and nonmyristoylated GCAP-2 as membrane insertion of the myristoyl chain should release a significant amount of free energy. A number of studies addressed the insertion of lipid-modified proteins and peptides into membranes as reviewed before (Brunsveld et al. 2009; McLaughlin and Aderem 1995; Murray et al. 1997; Silvius 2002). Basically, the interaction of lipidated proteins is governed by thermodynamics yielding a favorable ΔG^0 of -3.45 kJ/mol per membrane-inserted methylene group plus an entropy penalty on the order of $T\Delta S = 15$–20 kJ/mol (Tanford 1980). Therefore, simple binding measurements may provide insights into the question of whether or not the GCAP myristoyl chain is involved in membrane binding.

Our binding measurements showed that both myristoylated and nonmyristoylated GCAP-2 binds to membranes with rather high affinity. However, the difference in the binding energies between those two proteins is only $\Delta\Delta G^0 = -3.2$ kJ/mol. This insignificant difference clearly is too small to be explained by membrane insertion of the protein-bound myristoyl chain. According to data for the partitioning of fatty acids into *n*-heptane, for myristic acid, a value on the order of -25 to -30 kJ/mol is expected (Tanford 1980). This should be the order of magnitude for the $\Delta\Delta G^0$ between membrane binding of nonmyristoylated and myristolyated GCAP-2, which was not observed. This discrepancy could indeed mean that the myristoyl chain of GCAP-2 is not involved in membrane binding of the molecule and could actually remain buried inside the hydrophobic interior of the molecule upon binding.

In contrast, the measured ^{2}H solid-state NMR spectra of the myristoyl chain of GCAP-2 clearly show that the myristoyl moiety is incorporated into the membrane when GCAP-2 is bound to POPC liposomes. This is observed both in the presence and in the absence of Ca^{2+}. Membrane insertion of the myristoyl chain was also seen for GCAP-2 binding to DMPC and a more physiological membrane mix before (Vogel et al. 2007a). These results clearly mean that the myristoyl chain of GCAP-2 is permanently inserted into the membrane upon binding.

One suggestion to reconcile the observation that the myristoyl chain of GCAP-1 was buried inside the protein in the crystal with the result that it inserts into the membrane when present is that the myristoyl chain of GCAP is released from the protein interior upon membrane approach. This means that in the absence of membranes, the soluble GCAP protein would feature the myristoyl chain buried inside the hydrophobic pocket as seen for GCAP-1 in the crystal structure. Such a conformation would be thermodynamically favorable as a water-exposed fatty acid would represent an energetically unfavorable structure. Upon GCAP approaching the membrane, which would be driven by the insertion of hydrophobic residues into the membrane or perhaps by electrostatic interactions, the myristoyl chain would then have to be released from the protein interior in order to insert into the membrane. Such a chain extrusion process would require some conformational changes of the protein as previously observed for recoverin (Ames et al. 1997).

In order to see if similar conformational changes would occur for GCAP-2, we carried out solution NMR experiments. First, we compared nonmyristoylated and myristoylated GCAP-2 in the absence of detergents. The observed differences in the ^{1}H-^{15}N HSQC spectra indicated that the presence of the myristoyl chain has some influence on protein structure. However we could not observe any relevant shifts of the peaks relating to the N-terminal amino acids we were able to assign. This would suggest that the N-terminus of GCAP-2 has a similar fold in the

myristoylated and the nonmyristoylated form of the protein. A number of chemical shift changes of unassigned resonances were noticeable, probably caused by the myristic acid influencing the chemical shifts of nearby amino acids. When the crystal structure of GCAP-1 was solved, the authors found the myristic acid in a hydrophobic pocket. Although we have not directly investigated the localization of the myristoyl chain in the protein, our data do not disagree that this could also be the case for GCAP-2 in aqueous solution. Burying the myristic acid inside a hydrophobic pocket should indeed be energetically favorable for the protein in aqueous solution without membranes/micelles in range or in the environment of a protein crystal. Exposing the hydrophobic myristoyl chain to the water would be thermodynamically unfavorable; furthermore an exposed myristic acid would potentially disturb crystal packing. However, the ^{2}H NMR spectrum of deuterated myristoylated GCAP-2 did show a highly mobile myristoyl chain at 50 wt% hydration. This would suggest that this chain is rather free to move under these circumstances.

This picture changes, however, when membranes or detergent micelles are present. Our NMR data strongly suggest that the myristoyl chain is inserted into the hydrophobic interior of membranes or micelles when present. In agreement with this, the comparison of the ^{1}H-^{15}N HSQC spectra of myristoylated and nonmyristoylated GCAP-2 in the presence of 20 mM DPC showed mainly differences in the N-terminal region, which we were able to assign. We interpret these differences to occur upon insertion of the myristoyl chain into the micelles. The majority of the remaining signals, however, are not altered, suggesting that the structural changes necessary for this conformational change are moderate.

It should be mentioned that our discussion is based on the crystal structure of GCAP-1, our results, however, pertain to GCAP-2. While both proteins are very homologous, subtle differences between the structures of their activating domains have been proposed (Olshevskaya et al. 1997). However, there is also an argument that suggests that the myristoyl moiety of GCAP-2 could be buried inside the protein in the absence of membranes: although the presence of the myristoyl group makes no significant difference in the membrane binding energy of the GCAPs, the insertion of the myristoyl chain into the membrane should have released about −25 to −30 kJ/mol free energy. Since such an energy was not measured, one would assume that the ΔG^{0} of the unbound protein with the myristoyl chain inside would have a similar value as the membrane-bound protein with the chain inserted into the membrane, not counting the free energy gain of protein binding by local electrostatic interactions and insertion of hydrophobic residues. In other words, we propose that the hydrophobic environment of the membrane interior is similar to the hydrophobic environment of the protein interior so there is only a small free energy change associated with membrane insertion. Therefore, upon membrane binding, GCAP-2 would have to release the myristoyl chain from its binding pocket in an energetically unfavorable process, but this energy penalty is compensated by the free energy gain of membrane insertion of the chain. This would explain why myristoylated and nonmyristoylated GCAP-2 show very similar binding energies to phospholipid membranes.

In conclusion, we provide experimental data that support a model according to which soluble GCAP-2 protein features the myristoyl moiety sequestered inside a hydrophobic binding site of the protein, as shown in the crystal structure for GCAP-1. Upon membrane binding of the protein, this chain is inserted into the bilayer. The free energy gain of insertion is taken up by the less optimal protein conformation at the membrane surface that results from releasing the myristoyl chain to the membrane. This means that the thermodynamic energy difference between the state in which the myristoyl chain is buried inside a hydrophobic pocket and the state in which it is inserted into the membrane is negligibly small. But when the protein binds to the membrane (via another membrane binding side), the local concentration of lipids favors the insertion of the myristoyl moiety into the membrane (Penk et al. 2011).

One interesting aspect to investigate in the future would be the question of whether this exposure and membrane insertion of the myristoyl chain, with the subsequently occurring change in the protein structure, is necessary for the activation of the GC. This is suggested by studies from literature (Hwang and Koch 2002b; Olshevskaya et al. 1997), which revealed that the myristoyl moiety of GCAP-2 does not contribute to the membrane binding but leads to an increase in maximum GC activation.

Acknowledgments This work was supported by a grant from the Deutsche Forschungsgemeinschaft (DFG, HU 720/10-1). M.K. and J.B. were supported by grants from DFG (SFB 610) and J.B. by the Exzellenznetzwerk Biowissenschaften of Sachsen-Anhalt. J.B. thanks the European Development Fund of the European Union.

References

Ames JB, Ishima R, Tanaka T, Gordon JI, Stryer L, Ikura M (1997) Molecular mechanics of calcium-myristoyl switches. Nature 389:198–202

Ames JB, Dizhoor AM, Ikura M, Palczewski K, Stryer L (1999) Three-dimensional structure of guanylyl cyclase activating protein-2, a calcium-sensitive modulator of photoreceptor guanylyl cyclases. J Biol Chem 274:19329–19337

Ames JB, Hamasaki N, Molchanova T (2002) Structure and calcium-binding studies of a recoverin mutant (E85Q) in an allosteric intermediate state. Biochemistry 41:5776–5787

Barre P, Eliezer D (2006) Folding of the repeat domain of tau upon binding to lipid surfaces. J Mol Biol 362:312–326

Brunsveld L, Waldmann H, Huster D (2009) Membrane binding of lipidated Ras peptides and proteins—the structural point of view. Biochim Biophys Acta 1788:273–288

Burgoyne RD, Weiss JL (2001) The neuronal calcium sensor family of Ca^{2+}-binding proteins. Biochem J 353:1–12

Casey PJ (1995) Protein lipidation in cell signaling. Science 268: 221–225

Chen PS, Toribara TY, Warner H (1956) Microdetermination of phosphorus. Anal Chem 28:1756–1758

Davis JH, Jeffrey KR, Bloom M, Valic MI, Higgs TP (1976) Quadrupolar echo deuteron magnetic resonance spectroscopy in ordered hydrocarbon chains. Chem Phys Lett 42:390–394

Delaglio F, Grzesiek S, Vuister GW, Zhu G, Pfeifer J, Bax A (1995) NMR pipe—a multidimensional spectral processing system based on Unix pipes. J Biomol NMR 6:277–293

Demar JC, Rundle DR, Wensel TG, Anderson RE (1999) Heterogeneous N-terminal acylation of retinal proteins. Prog Lipid Res 38:49–90

Dizhoor AM, Olshevskaya EV, Henzel WJ, Wong SC, Stults JT, Ankoudinova I, Hurley JB (1995) Cloning, sequencing, and expression of a 24-KDa Ca^{2+}-binding protein activating photoreceptor guanylyl cyclase. J Biol Chem 270:25200–25206

Duronio RJ, Jackson-Machelski E, Heuckeroth RO, Olins PO, Devine CS, Yonemoto W, Slice LW, Taylor SS, Gordon JI (1990) Protein N-myristoylation in *Escherichia coli*: reconstitution of a eukaryotic protein modification in bacteria. Proc Natl Acad Sci USA 87:1506–1510

Frins S, Bönigk W, Müller F, Kellner R, Koch KW (1996) Functional characterization of a guanylyl cyclase-activating protein from vertebrate rods—cloning, heterologous expression, and localization. J Biol Chem 271:8022–8027

Gonzales-Horta A, Andreu D, Morrow MR, Perez-Gil J (2008) Effects of palmitoylation on dynamics and phospholipid-bilayer-perturbing properties of the N-terminal segment of pulmonary surfactant protein SP-C, as revealed by ^{2}H-NMR. Biophys J 95:2308–2317

Gorczyca WA, Gray-Keller MP, Detwiler PB, Palczewski K (1994) Purification and physiological evaluation of a guanylate cyclase activating protein from retinal rods. Proc Natl Acad Sci USA 91:4014–4018

Haynes LP, Burgoyne RD (2008) Unexpected tails of a Ca^{2+} sensor. Nat Chem Biol 4:90–91

Hope MJ, Bally MB, Webb G, Cullis PR (1985) Production of large unilamellar vesicles by a rapid extrusion procedure. Characterization of size distribution, trapped volume, and ability to maintain a membrane potential. Biochim Biophys Acta 812:55–65

Hughes RE, Brzovic PS, Dizhoor AM, Klevit RE, Hurley JB (1998) Ca^{2+}-dependent conformational changes in bovine GCAP-2. Protein Sci 7:2675–2680

Huster D, Arnold K, Gawrisch K (1998) Influence of docosahexaenoic acid and cholesterol on lateral lipid organization in phospholipid membranes. Biochemistry 37:17299–17308

Huster D, Vogel A, Katzka C, Scheidt HA, Binder H, Dante S, Gutberlet T, Zschörnig O, Waldmann H, Arnold K (2003) Membrane insertion of a lipidated ras peptide studied by FTIR, solid-state NMR, and neutron diffraction spectroscopy. J Am Chem Soc 125:4070–4079

Hwang JY, Koch KW (2002a) Calcium- and myristoyl-dependent properties of guanylate cyclase-activating protein-1 and protein-2. Biochemistry 41:13021–13028

Hwang JY, Koch KW (2002b) The myristoylation of the neuronal Ca^{2+}-sensors guanylate cyclase-activating protein 1 and 2. Biochim Biophys Acta 1600:111–117

Imanishi Y, Yang L, Sokal I, Filipek S, Palczewski K, Baehr W (2004) Diversity of guanylate cyclase-activating proteins (GCAPs) in teleost fish: characterization of three novel GCAPs (GCAP4, GCAP5, GCAP7) from zebrafish (*Danio rerio*) and prediction of eight GCAPs (GCAP1-8) in pufferfish (*Fugu rubripes*). J Mol Evol 59:204–217

Kay LE, Keifer P, Saarinen T (1992) Pure absorption gradient enhanced heteronuclear single quantum correlation spectroscopy with improved sensitivity. J Am Chem Soc 114:10663–10665

Kobayashi M, Takamatsu K, Saitoh S, Noguchi T (1993) Myristoylation of hippocalcin is linked to its calcium-dependent membrane association properties. J Biol Chem 268:18898–18904

Korz DJ, Rinas U, Hellmuth K, Sanders EA, Deckwer WD (1995) Simple fed-batch technique for high cell density cultivation of *Escherichia coli*. J Biotechnol 39:59–65

Ladant D (1995) Calcium and membrane-binding properties of bovine neurocalcin-delta expressed in *Escherichia coli*. J Biol Chem 270:3179–3185

Ladokhin AS, Jayasinghe S, White SH (2000) How to measure and analyze tryptophan fluorescence in membranes properly, and why bother? Anal Biochem 285:235–245

Lafleur M, Fine B, Sternin E, Cullis PR, Bloom M (1989) Smoothed orientational order profile of lipid bilayers by ^{2}H-nuclear magnetic resonance. Biophys J 56:1037–1041

Liu ML, Mao XA, Ye CH, Huang H, Nicholson JK, Lindon JC (1998) Improved WATERGATE pulse sequences for solvent suppression in NMR spectroscopy. J Magn Reson 132:125–129

McFerran BW, Weiss JL, Burgoyne RD (1999) Neuronal Ca^{2+} sensor 1–characterization of the myristoylated protein, its cellular effects in permeabilized adrenal chromaffin cells, Ca^{2+}-independent membrane association, and interaction with binding proteins, suggesting a role in rapid Ca^{2+} signal transduction. J Biol Chem 274:30258–30265

McLaughlin S, Aderem A (1995) The myristoyl-electrostatic switch: a modulator of reversible protein-membrane interactions. Trends Biochem Sci 20:272–276

Murray D, Ben-Tal N, Honig B, McLaughlin S (1997) Electrostatic interaction of myristoylated proteins with membranes: simple physics, complicated biology. Structure 5:985–989

O'Callaghan DW, Burgoyne RD (2004) Identification of residues that determine the absence of a Ca^{2+}/myristoyl switch in neuronal calcium sensor-1. J Biol Chem 279:14347–14354

Olshevskaya EV, Hughes RE, Hurley JB, Dizhoor AM (1997) Calcium binding, but not a calcium-myristoyl switch, controls the ability of guanylyl cyclase-activating protein GCAP-2 to regulate photoreceptor guanylyl cyclase. J Biol Chem 272:14327–14333

Palmer AG, Cavanagh J, Wright PE, Rance M (1991) Sensitivity improvement in proton-detected 2-dimensional heteronuclear correlation NMR spectroscopy. J Magn Reson 93:151–170

Peitzsch RM, McLaughlin S (1993) Binding of acylated peptides and fatty acids to phospholipid vesicles: pertinence to myristoylated proteins. Biochemistry 32:10436–10443

Penk A, Muller M, Scheidt HA, Langosch D, Huster D (2011) Structure and dynamics of the lipid modifications of a transmembrane alpha-helical peptide determined by (2)H solid-state NMR spectroscopy. Biochim Biophys Acta 1808:784–791

Petrache HI, Dodd SW, Brown MF (2000) Area per lipid and acyl length distributions in fluid phosphatidylcholines determined by ^{2}H NMR spectroscopy. Biophys J 79:3172–3192

Reuther G, Tan K-T, Vogel A, Nowak C, Kuhlmann J, Waldmann H, Huster D (2006) The lipidated membrane anchor of the N-ras protein shows an extensive dynamics as revealed by solid-state NMR. J Am Chem Soc 128:13840–13846

Rudolph R, Böhm G, Lilie H, Jaenicke R (1997) Folding proteins. In: Creighton T (ed) Protein function: a practical approach. IRL Oxford University Press, Oxford, pp 57–99

Scheidt HA, Huster D (2009) Structure and dynamics of the myristoyl lipid modification of Src peptides determined by ^{2}H solid-state NMR spectroscopy. Biophys J 96:3663–3672

Schleucher J, Schwendinger M, Sattler M, Schmidt P, Schedletzky O, Glaser SJ, Sorensen OW, Griesinger C (1994) A general enhancement scheme in heteronuclear multidimensional NMR employing pulsed-field gradients. J Biomol NMR 4:301–306

Seelig J, Seelig A (1980) Lipid conformation in model membranes and biological membranes. Q Rev Biophys 13:19–61

Seo ES, Blaum BS, Vargues T, De CM, Deakin JA, Lyon M, Barran PE, Campopiano DJ, Uhrin D (2010) Interaction of human beta-defensin 2 (HBD2) with glycosaminoglycans. Biochemistry 49:10486–10495

Shen Y, Bax A (2007) Protein backbone chemical shifts predicted from searching a database for torsion angle and sequence homology. J Biomol NMR 38:289–302

Silvius JR (2002) Lipidated peptides as tools for understanding the membrane interactions of lipid-modified proteins. In: Simon SA, McIntosh TJ (eds) Peptide-lipid interactions. Elsevier, Amsterdam, pp 371–395

Stephen R, Palczewski K, Sousa MC (2006) The crystal structure of GCAP3 suggests molecular mechanism of GCAP-linked cone dystrophies. J Mol Biol 359:266–275

Stephen R, Bereta G, Golczak M, Palczewski K, Sousa MC (2007) Stabilizing function for myristoyl group revealed by the crystal structure of a neuronal calcium sensor, guanylate cyclase-activating protein 1. Structure 15:1392–1402

Tanaka T, Ames JB, Harvey TS, Stryer L, Ikura M (1995) Sequestration of the membrane-targeting myristoyl group of recoverin in the calcium-free state. Nature 376:444–447

Tanford C (1980) The hydrophobic effect: formation of micelles and biological membranes. Wiley, New York

Theisgen S, Scheidt HA, Magalhaes A, Bonagamba TJ, Huster D (2010) A solid-state NMR study of the structure and dynamics of the myristoylated N-terminus of the guanylate cyclase-activating protein-2. Biochim Biophys Acta 1798:266–274

Venable RM, Zhang Y, Hardy BJ, Pastor RW (1993) Molecular dynamics simulations of a lipid bilayer and of hexadecane: an investigation of membrane fluidity. Science 262:223–226

Vogel A, Katzka CP, Waldmann H, Arnold K, Brown MF, Huster D (2005) Lipid modifications of a ras peptide exhibit altered packing and mobility versus host membrane as detected by ^{2}H solid-state NMR. J Am Chem Soc 127:12263–12272

Vogel A, Schröder T, Lange C, Huster D (2007a) Characterization of the myristoyl lipid modification of membrane-bound GCAP-2 by ^{2}H solid-state NMR spectroscopy. Biochim Biophys Acta 1768:3171–3181

Vogel A, Tan K-T, Waldmann H, Feller SE, Brown MF, Huster D (2007b) Flexibility of ras lipid modifications studied by ^{2}H solid-state NMR and molecular dynamics simulations. Biophys J 93:2697–2712

Vogel A, Reuther G, Weise K, Triola G, Nikolaus J, Tan KT, Nowak C, Herrmann A, Waldmann H, Winter R, Huster D (2009) The lipid modifications of Ras that sense membrane environments and induce local enrichment. Angew Chem Int Ed Engl 48:8784–8787

Weiergraber OH, Senin II, Philippov PP, Granzin J, Koch KW (2003) Impact of N-terminal myristoylation on the Ca^{2+}-dependent conformational transition in recoverin. J Biol Chem 278:22972–22979

White SH, Wimley WC (1999) Membrane protein folding and stability: physical principles. Annu Rev Biophys Biomol Struct 28:319–365

Zozulya S, Stryer L (1992) Calcium-myristoyl protein switch. Proc Natl Acad Sci USA 89:11569–11573